Behavioral/Cognitive

Neurophysiology of Perceptual Decision-Making and Its Alterations in Attention-Deficit Hyperactivity Disorder

Mana Biabani,[1] Kevin Walsh,[1] Shou-Han Zhou,[2] Joseph Wagner,[3] Alexandra Johnstone,[1] Julia Paterson,[1] Beth P. Johnson,[1] Natasha Matthews,[3] Gerard M. Loughnane,[4] Redmond G. O'Connell,[5] and Mark A. Bellgrove[5]

[1]The Turner Institute for Brain and Mental Health, School of Psychological Sciences, Monash University, Melbourne, Victoria 3800, Australia, [2]School of Engineering, Cardiff University, Cardiff, Cardiff CF24 3AA, Wales, United Kingdom, [3]Queensland Brain Institute, University of Queensland, Brisbane, Queensland 4067, Australia, [4]School of Psychology, Dublin City University, Dublin 9, Ireland, and [5]Trinity College Institute of Neuroscience and School of Psychology, Trinity College Dublin, Dublin D02 PX31, Ireland

Despite the prevalence of attention-deficit hyperactivity disorder (ADHD), efforts to develop a detailed understanding of the neuropsychology of this neurodevelopmental condition are complicated by the diversity of interindividual presentations and the inability of current clinical tests to distinguish between its sensory, attentional, arousal, or motoric contributions. Identifying objective methods that can explain the diverse performance profiles across individuals diagnosed with ADHD has been a long-held goal. Achieving this could significantly advance our understanding of etiological processes and potentially inform the development of personalized treatment approaches. Here, we examine key neuropsychological components of ADHD within an electrophysiological (EEG) perceptual decision-making paradigm that is capable of isolating distinct neural signals of several key information processing stages necessary for sensory-guided actions from attentional selection to motor responses. Using a perceptual decision-making task (random dot motion), we evaluated the performance of 79 children (aged 8–17 years) and found slower and less accurate responses, along with a reduced rate of evidence accumulation (drift rate parameter of drift diffusion model), in children with ADHD ($n = 37$; 13 female) compared with typically developing peers ($n = 42$; 18 female). This was driven by the atypical dynamics of discrete electrophysiological signatures of attentional selection, the accumulation of sensory evidence, and strategic adjustments reflecting urgency of response. These findings offer an integrated account of decision-making in ADHD and establish discrete neural signals that might be used to understand the wide range of neuropsychological performance variations in individuals with ADHD.

Key words: **ADHD; attention; drift diffusion model; EEG; evidence accumulation; perceptual decision-making**

Significance Statement

The efficacy of diagnostic and therapeutic pathways in attention-deficit hyperactivity disorder (ADHD) is limited by our incomplete understanding of its neurological basis. One promising avenue of research is the search for basic neural mechanisms that may contribute to the variety of cognitive challenges associated with ADHD. We developed a mechanistic account of differences in a fundamental cognitive process by integrating across neurocognitive, neurophysiological (i.e., EEG), and computational levels of analysis. We detected distinct neural changes in ADHD that explained altered performance (e.g., slowed and less accurate responses). These included changes in neural patterns of attentional selection, sensory information processing, and response preparation. These findings enhance our understanding of the neurophysiological profile of ADHD and may offer potential targets for more effective, personalized interventions.

Received March 11, 2024; revised Jan. 12, 2025; accepted Jan. 22, 2025.

Author contributions: N.M., R.G.O., and M.B. designed research; M.B., J.W., A.J., and J.P. performed research; M.B., B.P.J., G.M.L., and M.A.B. contributed unpublished reagents/analytic tools; M.B., K.W., S-H.Z., and G.M.L. analyzed data; M.B. wrote the paper.

This work is supported by grants from the National Health and Medical Research Council (NHMRC) of Australia to M.A.B (s2010899; 2025415).

The authors declare no competing financial interests.

Correspondence should be addressed to Mana Biabani at mana.biabani@monash.edu or Mark A. Bellgrove at Mark.Bellgrove@monash.edu.

https://doi.org/10.1523/JNEUROSCI.0469-24.2025

Introduction

Attention-deficit hyperactivity disorder (ADHD) is a prevalent childhood-onset condition characterized by persistent inattentive, hyperactive, and/or impulsive symptoms that significantly impact social relationships and quality of life (Barkley, 1997; Nigg, 2013; Sciberras et al., 2022). Early attempts to identify the neuropsychological characteristics of ADHD focused primarily on differences in higher-level cognitive processes associated with executive functioning such as response inhibition, working

memory, and cognitive flexibility (Pennington and Ozonoff, 1996; Barkley, 1997; Sergeant et al., 2002). However, ADHD is now recognized as a complex, heterogeneous, and multifactorial condition with contributions spanning multiple levels of processing (Sergeant et al., 2003; Willcutt et al., 2005; Coghill et al., 2014), including basic perceptual (Kim et al., 2014; Gonen-Yaacovi et al., 2016; Mihali et al., 2018; Panagiotidi et al., 2018) and neuromotor processes (Hurks et al., 2005; Rommelse et al., 2008; Kaiser et al., 2015; Goulardins et al., 2017). This raises the possibility that differences in higher-level processes may actually be the consequence of changes in more basic mechanisms that support downstream functions (Rommelse et al., 2007). Many of these component processes have been identified based on hallmark differences in performance on reaction time tasks, where ADHD participants typically exhibit reduced accuracy and slower, more variable reaction times (Bellgrove et al., 2005; Johnson et al., 2007; Karalunas and Huang-Pollock, 2013). However, since these behavioral outputs are the product of multiple processes (e.g., sensory encoding, evidence accumulation, motor preparation, urgency, decision bias, and strategy), it is difficult to develop mechanistic accounts based on behavioral differences alone.

Sequential sampling models, like the drift diffusion model (DDM; Ratcliff and McKoon, 2008), provide a powerful theoretical framework that can help to disentangle these influences by recovering latent psychological processes from their behavioral output (Forstmann et al., 2016). These models conceptualize decision-making as a dynamic process of the accumulation of noisy sensory evidence over time until a decision threshold is reached and a response is initiated. Studies that have applied these models to the data of children with ADHD have identified slower accumulation of sensory evidence (reflected in a reduced drift rate parameter; Mowinckel et al., 2015), no differences in bound adjustments (Mulder et al., 2010), and mixed evidence for differences in the nondecision time parameter which incorporates delays associated with stimulus encoding and motor execution (Huang-Pollock et al., 2012, 2017; Karalunas et al., 2012, 2014, 2018). Although these models highlight distinct decision-making mechanisms that are potentially altered in ADHD, they offer little insight into the underlying neurophysiological mechanisms.

Building on foundational work in monkey neurophysiology (Gold and Shadlen, 2007; Hanks and Summerfield, 2017), human research now capitalizes on EEG paradigms to decompose simple decisions into their neural components, noninvasively mapping key information processing stages in decision-making (O'Connell and Kelly, 2021). These neural signals index processes representing candidate differences in decision-making in ADHD, including pretarget attentional engagement (alpha power; Kelly and O'Connell, 2013), early attentional selection (N2c; Loughnane et al., 2016), dynamic urgency (contingent negative variation; CNV; Devine et al., 2019), and evidence accumulation (centroparietal positivity; CPP). As the neural marker of the evidence accumulation process, the behavior of CPP is consistent with the predictions of sequential sampling models. Specifically, its build-up rate scales with evidence strength and predicts reaction time, while its peak amplitude, occurring at response, varies with prior knowledge and time pressure (Kelly and O'Connell, 2015; O'Connell et al., 2018). There is also compelling evidence linking CPP onset to nondecision time (Loughnane et al., 2016).

Here, we sought to develop an integrated account of the neurophysiology of ADHD by linking these distinct EEG signals to mechanisms associated with performance of a perceptual decision-making task. We first aimed to establish linkages between EEG metrics of decision-making with behavior and DDM parameters in children with and without ADHD. Second, we aimed to characterize the dynamics of decision-making signals in ADHD, developing a mechanistic account that captures individual variations in performance. This comprehensive analysis allowed us to explore the neural, cognitive, and computational factors that govern decision-making in the context of ADHD.

Materials and Methods

Participants. The study included a total of 79 right-handed individuals with normal or corrected-to-normal vision who were aged between 8 and 17 years, comprising 37 participants with ADHD (13 female; $\text{Mean}_{age} = 13.45$ years $\pm \text{SD}_{age} = 2.026$) and 42 typically developing controls (18 female; $\text{Mean}_{age} = 13.46$ years $\pm \text{SD}_{age} = 1.93$). Data were collected at the University of Queensland (UQ; $n = 58$) and Monash University ($n = 21$) in Australia following identical experimental protocols. Ethical approval was obtained from the human research ethics committees of both universities, and the study was conducted in accordance with approved guidelines. For the ADHD group, inclusion criteria required previous diagnosis by a specialist (e.g., psychiatrist or pediatrician), confirmed using the Anxiety Disorders Interview Schedule for DSM-IV (A-DISC child version for UQ participants) or The Development and Well-being Assessment (DAWBA, for Monash participants) and the Global Index on the Conners' Parent Rating Scale-Revised: Long Version (CPRS-R: L; T-Score >65 from the mean). The participants with ADHD completed a 48 h washout of ADHD-related medications before testing. Typically developing children were free of clinical diagnoses and had Conners' Global Index T-Scores <65. Informed consent from parents or guardians and assent was obtained from the participant prior to testing. This study originally recruited 85 individuals but six were excluded from the analyses: three due to the lack of research-standard clinical evaluations (e.g., semistructured interview) to confirm their group allocation and three due to recording issues (i.e., frequent pauses during the task, highly artifactual EEG recordings, and/or excessive cap movement). Figure 1 presents the clinical characteristics of the individuals in the two groups.

Experimental protocol. Participants were seated in a darkened sound-attenuated room positioned at a viewing distance of ~56 cm from a 21 inch CRT monitor (resolution, 1,024 × 768; refresh rate. 85 Hz) and instructed to perform a bilateral random dot motion perceptual decision-making task. The task was run through MATLAB's psychophysics toolbox extension on a 32 bit Windows XP computer (Brainard and Vision, 1997). A chin rest was employed to stabilize participants' heads and maintain a constant visual angle throughout the task. An EyeLink 1000 eye tracking system (SR Research) was used to monitor gaze at fixation.

In this task (Fig. 2), participants fixated on a centrally presented 5 × 5-pixel square dot while simultaneously monitoring two circular patches, one per hemifield. These peripheral patches were 8° in diameter and contained 150 randomly moving 6 × 6 pixel dots. The center of each patch was situated 4° below and 10° to the left or right of the central fixation dot to maintain an optimum visual angle for both hemifields. At pseudorandom intertarget intervals of either 3.06, 5.17, or 7.29 s, during which the incoherent motion was continuously displayed, a subset of the dots transitioned to coherent downward motion for 1.88 s (Stefanac et al., 2021). These dots were randomly selected to move downward by 0.282° per frame (6° per second). Trials were marked by each occurrence of coherent (target) motion within the continuous incoherent background. The coherent downward motion occurred with equal probability in either the left or right hemifield patch. Participants were instructed to respond promptly by pressing both mouse buttons simultaneously with their thumbs upon detecting the downward motion, employing a double thumb click. The stimulus was displayed for the entire duration of 1.88 s, regardless of when the response occurred. To capture robust accuracy and reaction time contrasts between groups, a relatively low coherence

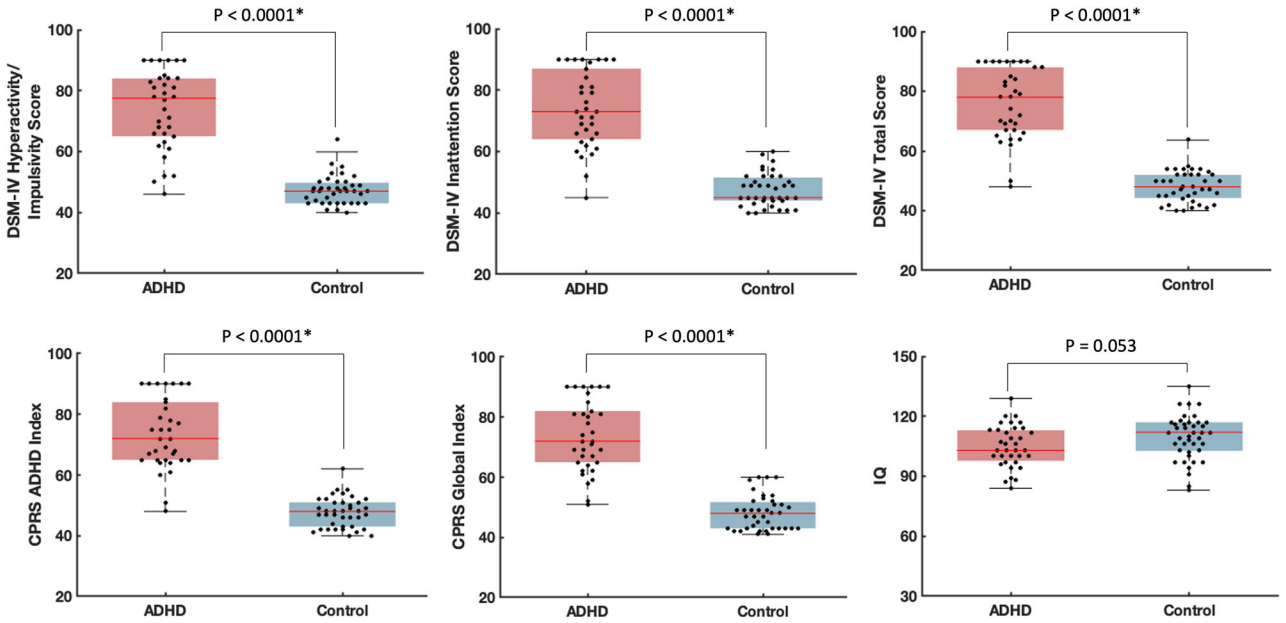

Figure 1. Clinical characteristics of participants in each group. P, *p* value from Wilcoxon signed rank test comparing the two groups. Every data point in the box and whisker plots corresponds to the clinical score for one individual. The shaded boxes indicate the range between the 25th and 75th percentiles of the scores, whereas the red horizontal lines inside the boxes represent the median score. * indicates statistically significant differences between groups.

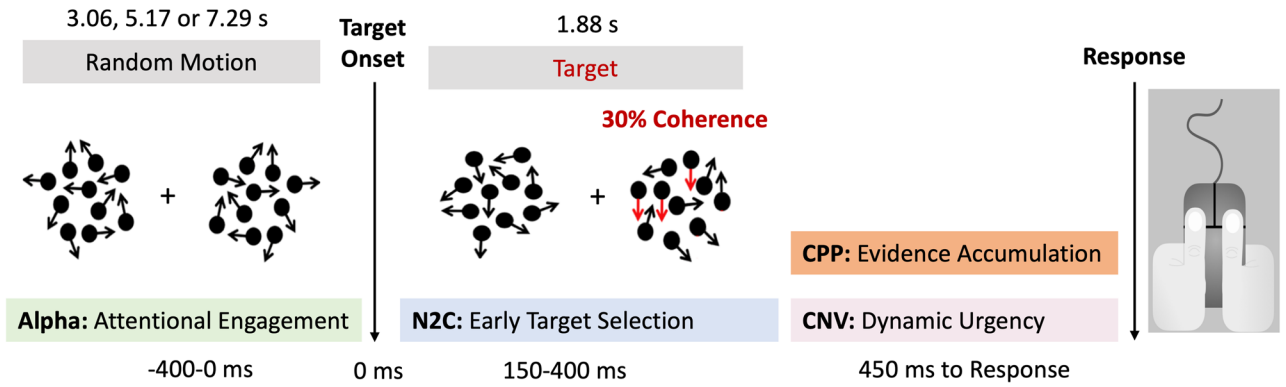

Figure 2. Depiction of the random dot motion detection task and the obtained neural measures. Note that in the actual task, white dots were presented on a black background. Here, we have adjusted the visualization for better clarity.

level of 30% was chosen for this task, deviating from previous studies using the same paradigm (Loughnane et al., 2016; Stefanac et al., 2021). Participants completed 200 trials of the task, divided into 10 blocks of 20 coherent motion trials each, with intermittent breaks to reduce fatigue.

EEG acquisition and preprocessing. Continuous EEG data were acquired from 64 scalp electrodes (10–10 layout) using BioSemi Active II (Neurospec) digitized at 1,024 Hz (at the University of Queensland) or a BrainAmp DC system (Brain Products) digitized at 500 Hz (at Monash University). Data were analyzed using custom scripts in MATLAB (The MathWorks) and EEGLAB toolbox (Delorme and Makeig, 2004). EEG recordings from the two locations were combined by downsampling the data collected in Queensland to 500 Hz. Signals were low-pass filtered up to a 35 Hz cutoff using Hamming windowed-sinc FIR filter, and no high-pass filter was applied. Noisy channels were then interpolated using spherical spline interpolation and the data were rereferenced to the common average. Target epochs were extracted using a window of −800 to 1,880 ms around the onset of the target stimulus (coherent motion) and baseline corrected at −100 to 0 ms. The behavioral measures of reaction time (RT) and accuracy were extracted as the average time to respond to a target in milliseconds (ms) and the percentage of correctly identified targets, respectively. Trials were rejected if any of the following occurred: (1) the central gaze fixation was broken by blinking or vertical/horizontal eye movement >3°; (2) recordings from any electrode exceeded ±100 μV; (3) RTs were faster than 200 ms (pre-emptive responses) or slower than 1,880 ms (responses after the offset of coherent motion). Missed targets were defined as either responses that took longer than 1,880 ms or complete absence of responses. Hit rate was measured as the percentage of trials with valid responses.

ERPs for each individual were extracted from the average of single-trial epochs. For each individual, we isolated four distinct and previously validated EEG signatures of decision-making processes (Brosnan et al., 2020): pretarget attentional engagement (alpha power), early target selection (N2c peak latency and amplitude (Loughnane et al., 2016), evidence accumulation (CPP onset latency, slope, and amplitude (O'Connell et al., 2012; McGovern et al., 2018; Steinemann et al., 2018), and dynamic urgency (CNV slope and amplitude (Devine et al., 2019). Pretarget alpha power was computed using the temporal spectral evolution approach, in which all epochs (−1,000 to 2,080 ms) were bandpass filtered at 8–13 Hz, rectified, and trimmed by 200 ms at both ends of the

epoch (target epoch, −800:1,880 ms) to eliminate filter warm-up artifacts. Subsequently, the data were smoothed by averaging within a 100 ms moving window shifting forward in 50 ms steps throughout each epoch. Mean alpha power was extracted bilaterally at peak electrodes—PO3/PO7 (left hemisphere) and PO4/PO8 (right hemisphere)—from 400 to 0 ms prior to the target onset and was baseline corrected using the period of 700–400 ms before the target onset (Brosnan et al., 2020). For N2c components, peak negative amplitude was measured contralateral to the target hemifield, from electrodes P7 and P8 between 150 and 400 ms post target onset (Stefanac et al., 2021). CPP was extracted from the average of the potentials recorded at the peak electrodes—Pz and POz—and CNV was measured at FCz. The amplitude of CPP and CNV was determined by calculating the mean signal amplitude within the same 100 ms window preceding the response. The slope of CNV was estimated using the same time window. The maximum increase in negativity was detected using the second derivative method (ADHD = −84 ms, Control = −56 ms, averaging at −70 ms), and the slope of a line fitted to this window (−70 ms to response) was defined as the CNV slope. CPP onset latency, marking the beginning of neural evidence accumulation, was derived by performing point-by-point one-sample *t* tests against zero over the stimulus-locked trials for each individual. The onset was defined as the first point in time when the amplitude reached the significance level of 0.05 for 25 consecutive samples (Foxe and Simpson, 2002). The build-up rate of the CPP was measured as the slope of a straight line fitted to the response-locked signal at −450 to −50 ms (Loughnane et al., 2016; Zhou et al., 2021). The variation of the task used in this study, involving double thumb clicks, did not allow us to extract motoric signals, such as lateralized beta activity.

Drift diffusion modeling. The DDM was fitted to the behavior of all participants (both ADHD and typically developing children) at an individual level (Ratcliff et al., 2018). The response time data for each individual was first split into six equal speed bins defined by five quantiles (0.1, 0.3, 0.5, 0.7, and 0.9), resulting in four 20% bins and two 10% bins. Together with a single bin containing the number of missed responses, these seven bins were then used to fit the DDM using the G-square method of the hDDM package (Wiecki et al., 2013; Ratcliff et al., 2016; de Gee et al., 2020). This method is a variant of the chi-squared method and was chosen for its efficiency, the availability of significant trial data for each individual, its robustness to outliers, and its success in previous similar experiments (Ratcliff et al., 2016; Myers et al., 2022). The G-square statistics is defined as follows:

$$G^2 = 2\sum_{i=1}^{7} O_i \ln\left(\frac{O_i}{E_i}\right),$$

where $i \in N$ represents the quantile number. The variable $O_i \in R$ represents the number of observations in each bin (in this case: 0.1, 0.2, 0.2, 0.2, 0.2, and 0.1 of the total number of observations), and $E_i \in R$ represents the expected number of observations in each bin, as predicted by the DDM. The expected number of observations is determined by first inserting the simulated response times into a DDM cumulative probability function to obtain the expected cumulative probability up to the five quantiles. Then, the proportion of simulated responses between each quantile is calculated by subtracting the cumulative probabilities for each successive quantile from the next highest quantile. This proportion is then multiplied by the total number of observations to obtain the expected frequencies. The DDM parameters *a*, *v*, and *t* were determined by minimizing the G-square statistic using the modified Powell method (Powell, 1964). To obtain the best fitting model, 1,000 different runs of the optimization were performed with starting points chosen from a normal distribution with a mean of the best parameter value and a standard deviation of 0.5. The fitted DDM assumed that the decision threshold (*a*), drift rate (*v*), and nondecision time (*t*) varied between subjects. A chi-squared statistical procedure was then done to assess the goodness of fit for the model on each individual subject. The identified model for each subject was used to generate 1,000 samples of response times and accuracy. Histograms of the simulated and experimental data were then constructed across 20 equal bins. Since there were three DDM parameters fitted through the model, the resulting comparison means that there are 26 degrees of freedom resulting in a critical chi-squared statistic of ∼38.8. The obtained chi-square values were lower than the critical value (range, 1.16 to 7.01), resulting in a *p* value of approximately 1 for all individuals. This suggests that the model produces data that are very good fits with the experimental data. Further details can be found in Ratcliff et al. (2018) and de Gee et al. (2020).

Statistical analysis. Significant outliers were winsorized to the 5th percentile (for the lower outliers) and the 95th percentile (for the upper outliers) in each participant group to improve normality of distributions. CPP onset could not be detected for five individuals in each group due to noisy signals, so the missing values were replaced with the group median.

First, we adopted a hierarchical regression approach to investigate the association between the EEG signals (alpha power, N2c, CPP, and CNV), and both behavioral (RT, miss rate, and hit rate) and DDM (drift rate, decision threshold, nondecision time) outcomes. Separate hierarchical linear regression models were applied for each behavioral and DDM measure as a function of the EEG signals using data from all individuals, combining both groups. Diagnostic analyses confirmed that key assumptions for linear regression modeling were satisfied. The residuals did not exhibit skewness, as indicated by the normal P–P plots, confirming normality. Additionally, scatterplots of standardized residuals confirmed homoscedasticity. Multicollinearity was not present, with tolerance values above 0.1, VIFs below 10, and Pearson's correlation coefficients among predictors (EEG signals) <0.9. EEG components were sequentially entered into the regression models, following the temporal order of the perceptual decision-making processes: pretarget attentional engagement (alpha power), early target selection (N2c peak latency and amplitude), evidence accumulation (CPP onset, slope, and amplitude), and dynamic urgency (CNV slope and amplitude). This hierarchical entry method allowed us to evaluate whether each individual neurophysiological signal contributed to the model fit for behavioral performance or DDM parameters beyond the preceding signals in the temporal sequence. The independent power of each neurophysiological signal to predict behavior was also evaluated. Next, Spearman's partial correlation analyses were employed, controlling for the effects of group (ADHD, control), age, and recruitment site (Monash, UQ), to evaluate the magnitude and orientation of the relationship between EEG components and both behavioral outcomes and DDM parameters.

To determine any differences in decision-making processes in ADHD versus typically developing children, a multivariate analysis of covariance (MANCOVA) was conducted to compare the two groups on behavioral measures (RT, miss rate, and hit rate); EEG signatures including alpha (power), N2c (peak latency, amplitude), CPP (onset, amplitude, slope), and CNV (amplitude, slope); and the DDM parameters (drift rate, decision threshold, nondecision time), while controlling for the effect of age and recruitment site. We also examined whether the EEG signals were related to ADHD symptom scores while accounting for the effects of group, age, and site. For this analysis we employed five separate linear regression models, followed by false discovery rate (FDR) adjustment, each with one ADHD symptom domain as the dependent variable (i.e., DSM-IV hyperactivity/impulsivity score, DSM-IV inattention score, DSM-IV total score, CPRS ADHD Index, CPRS Global Index), while EEG signatures were entered into the model hierarchically.

Results

We first examined the relationship between each EEG signal (alpha, N2c, CPP, and CNV) and variations in behavior using a hierarchical regression model. In the initial step of the model, group, site, and age were entered as nuisance variables. In the subsequent steps, we sequentially incorporated the neural markers of attentional engagement (alpha power), target selection (N2c: peak latency and amplitude), evidence accumulation (CPP: onset, amplitude, and slope), and dynamic urgency (CNV: amplitude and slope) into the model. This hierarchical methodology allowed us to control for the chronological order of neural processes in

perceptual decision-making and examine the incremental predictive power of different signals. Although the existing literature suggests connections between certain EEG signals and behavioral/DDM measures (Yau et al., 2021), we avoided making a priori assumptions about these relationships in our analysis. Instead, we systematically examined each component to evaluate their impact and uncover any latent patterns and interactions. In a similar study with a comparable design and analytical framework, a sample size of 72 participants was sufficient to detect meaningful effects across similar predictors [Cohen's $f^2 = 0.29$; Power = 88.86% (G * Power 3.1); Brosnan et al., 2023]. Building on this previous work, we determined that a sample size of 79 participants would ensure robust power for the current study.

Neural signals predicting variations in reaction time

The neural signatures of the decision process collectively accounted for a substantial 52% of the variance in RT. Adding each of the neural components resulted in a significant improvement in the model fit (alpha power: $R^2_{adj} = 0.21$, $F_{(4,74)} = 6.33$, $p < 0.001$; N2c latency: $R^2_{adj} = 0.21$, $F_{(5,73)} = 5.26$, $p < 0.001$; N2c amplitude: $R^2_{adj} = 0.21$, $F_{(6,72)} = 4.37$, $p < 0.001$; CPP onset: $R^2_{adj} = 0.32$, $F_{(7,71)} = 6.36$, $p < 0.001$; CPP slope: $R^2_{adj} = 0.46$, $F_{(8,70)} = 9.32$, $p < 0.001$; CPP amplitude: $R^2_{adj} = 0.53$, $F_{(9,69)} = 10.76$, $p < 0.001$; CNV slope: $R^2_{adj} = 0.53$, $F_{(10,68)} = 9.71$, $p < 0.001$; CNV amplitude: $R^2_{adj} = 0.52$, $F_{(11,67)} = 8.69$, $p < 0.001$). The analysis of coefficients revealed that alpha power (stand. $\beta = 0.18$, $t = 2.17$, $p = 0.034$) and all CPP components (onset: stand. $\beta = 0.45$, $t = 4.94$, $p < 0.001$; slope: stand. $\beta = -0.84$, $t = -4.67$, $p < 0.001$; amplitude: stand. $\beta = 0.56$, $t = 2.87$, $p = 0.007$) had independent predictive power for RT, highlighting their potential as robust markers of changes in decision-making processes.

Neural signals predicting variations in miss rate

The second model examined the neural predictors of miss rate and yielded comparable outcomes with those of RT. The EEG signals collectively accounted for 30% of variations in miss rate. All neural components significantly improved model fit (alpha power: $R^2_{adj} = 0.17$, $F_{(4,74)} = 5.14$, $p = 0.001$; N2c latency: $R^2_{adj} = 0.16$, $F_{(5,73)} = 4.08$, $p = 0.003$; N2c amplitude: $R^2_{adj} = 0.16$, $F_{(6,72)} = 3.54$, $p = 0.004$; CPP onset: $R^2_{adj} = 0.28$, $F_{(7,71)} = 5.26$, $p < 0.001$; CPP slope: $R^2_{adj} = 0.27$, $F_{(8,70)} = 4.69$, $p < 0.001$; CPP amplitude: $R^2_{adj} = 0.26$, $F_{(9,69)} = 4.11$, $p < 0.001$; CNV slope: $R^2_{adj} = 0.27$, $F_{(10,68)} = 3.86$, $p < 0.001$; CNV amplitude: $R^2_{adj} = 0.30$, $F_{(11,67)} = 3.99$, $p < 0.001$) but only CPP onset demonstrated independent predictive power for miss rate (stand. $\beta = 0.44$, $t = 3.96$, $p < 0.001$), underlying its significance in determining performance on this particular task.

Neural signals predicting variations in hit rate

In the third model, we explored the neural predictors of hit rate. The examined EEG metrics collectively accounted for 34% of the variance in hit rate. In line with the results from RT and miss rate, adding each metric substantially enhanced the model's overall fit (alpha power: $R^2_{adj} = 0.21$, $F_{(4,74)} = 6.03$, $p < 0.001$; N2c latency: $R^2_{adj} = 0.19$, $F_{(5,73)} = 4.78$, $p < 0.001$; N2c amplitude: $R^2_{adj} = 0.19$, $F_{(6,72)} = 4.09$, $p = 0.001$; CPP onset: $R^2_{adj} = 0.28$, $F_{(7,71)} = 5.41$, $p < 0.001$; CPP slope: $R^2_{adj} = 0.29$, $F_{(8,70)} = 4.91$, $p < 0.001$; CPP amplitude: $R^2_{adj} = 0.28$, $F_{(9,69)} = 4.32$, $p < 0.001$; CNV slope: $R^2_{adj} = 0.28$, $F_{(10,68)} = 3.97$, $p < 0.001$; CNV amplitude: $R^2_{adj} = 0.34$, $F_{(11,67)} = 4.62$, $p < 0.001$). CPP onset (stand. $\beta = -0.43$, $t = -4.003$, $p < 0.001$) and CNV measures (slope: stand. $\beta = -0.39$, $t = -2.27$, $p = 0.023$; amplitude: stand. $\beta = -0.39$, $t = -2.72$, $p = 0.008$) made significant individual contributions to the prediction of hit rate.

Together, these results provide compelling evidence that the EEG metrics of target selection (N2c), evidence accumulation (CPP), and dynamic urgency (CNV) collectively exhibit predictive power for decision-making performance across the three behavioral measures (RT, miss rate, hit rate). This underscores the importance of considering multiple neural components when investigating and interpreting decision-making processes. Although the neural signals showed varying contributions to each behavioral measure, CPP onset emerged as an independent predictor for performance variations across all the three measures. Figure 3 illustrates the relationships between CPP onset and performance, along with the Spearman's correlation coefficients.

Collective predictive power of neural metrics on DDM parameters

Next, we examined whether the EEG signatures of decision-making processes were associated with DDM parameters fitted to the behavioral measures by modeling each DDM parameter as a function of the EEG signals in hierarchical regression analysis. Group, age, and site were entered as nuisance factors at the first stage of each model.

Neural signals predicting variations in nondecision time (t)

Nondecision time refers to the combination of the time taken to encode the stimulus and the response execution occurring before and after evidence accumulation, respectively. The EEG signals collectively accounted for 30% of variations of the nondecision time parameter of the DDM and the model fit significantly improved by adding each of the neural components into the model (alpha power: $R^2_{adj} = 0.15$, $F_{(4,74)} = 4.40$, $p = 0.003$; N2c latency: $R^2_{adj} = 0.21$, $F_{(5,73)} = 5.10$, $p < 0.001$; N2c amplitude: $R^2_{adj} = 0.20$, $F_{(6,72)} = 4.23$, $p < 0.001$; CPP onset: $R^2_{adj} = 0.26$, $F_{(7,71)} = 4.97$, $p < 0.001$; CPP slope: $R^2_{adj} = 0.28$, $F_{(8,70)} = 4.82$, $p < 0.001$; CPP amplitude: $R^2_{adj} = 0.31$, $F_{(9,69)} = 4.93$, $p < 0.001$; CNV slope: $R^2_{adj} = 0.30$, $F_{(10,68)} = 4.38$, $p < 0.001$; CNV amplitude: $R^2_{adj} = 0.30$, $F_{(11,67)} = 4.02$, $p < 0.001$). The analysis of coefficients revealed that all CPP components (onset: stand. $\beta = 0.37$, $t = 3.33$, $p = 0.001$; slope: stand. $\beta = -0.58$, $t = -2.67$, $p = 0.009$; amplitude: stand. $\beta = 0.52$, $t = 2.14$, $p = 0.03$) had independent predictive power for nondecision time.

Neural signals predicting variations in drift rate (v)

Drift rate refers to the speed at which the process of evidence accumulation approaches one of the two decision boundaries. Similar to the nondecision time, the model fit for the drift rate parameter was significantly improved when each of the EEG metrics was added into the model. This model explained 30% of the variance in drift rate (alpha power: $R^2_{adj} = 0.20$, $F_{(4,74)} = 5.78$, $p < 0.001$; N2c latency: $R^2_{adj} = 0.26$, $F_{(5,73)} = 4.47$, $p < 0.001$; N2c amplitude: $R^2_{adj} = 0.25$, $F_{(6,72)} = 5.46$, $p < 0.001$; CPP onset: $R^2_{adj} = 0.28$, $F_{(7,71)} = 5.32$, $p < 0.001$; CPP slope: $R^2_{adj} = 0.27$, $F_{(8,70)} = 4.68$, $p < 0.001$; CPP amplitude: $R^2_{adj} = 0.27$, $F_{(9,69)} = 4.22$, $p < 0.001$; CNV slope: $R^2_{adj} = 0.28$, $F_{(10,68)} = 4.01$, $p < 0.001$; CNV amplitude: $R^2_{adj} = 0.30$, $F_{(11,67)} = 4.09$, $p < 0.001$). CPP onset (stand. $\beta = -0.30$, $t = -2.66$, $p = 0.001$) and CNV slope (stand. $\beta = 0.27$, $t = 2.13$, $p = 0.03$) accounted for independent variation in drift rate.

Neural signals predicting variations in response threshold (a)

Response threshold is the amount of accumulated evidence required for a decision to be made. EEG signals explained 22%

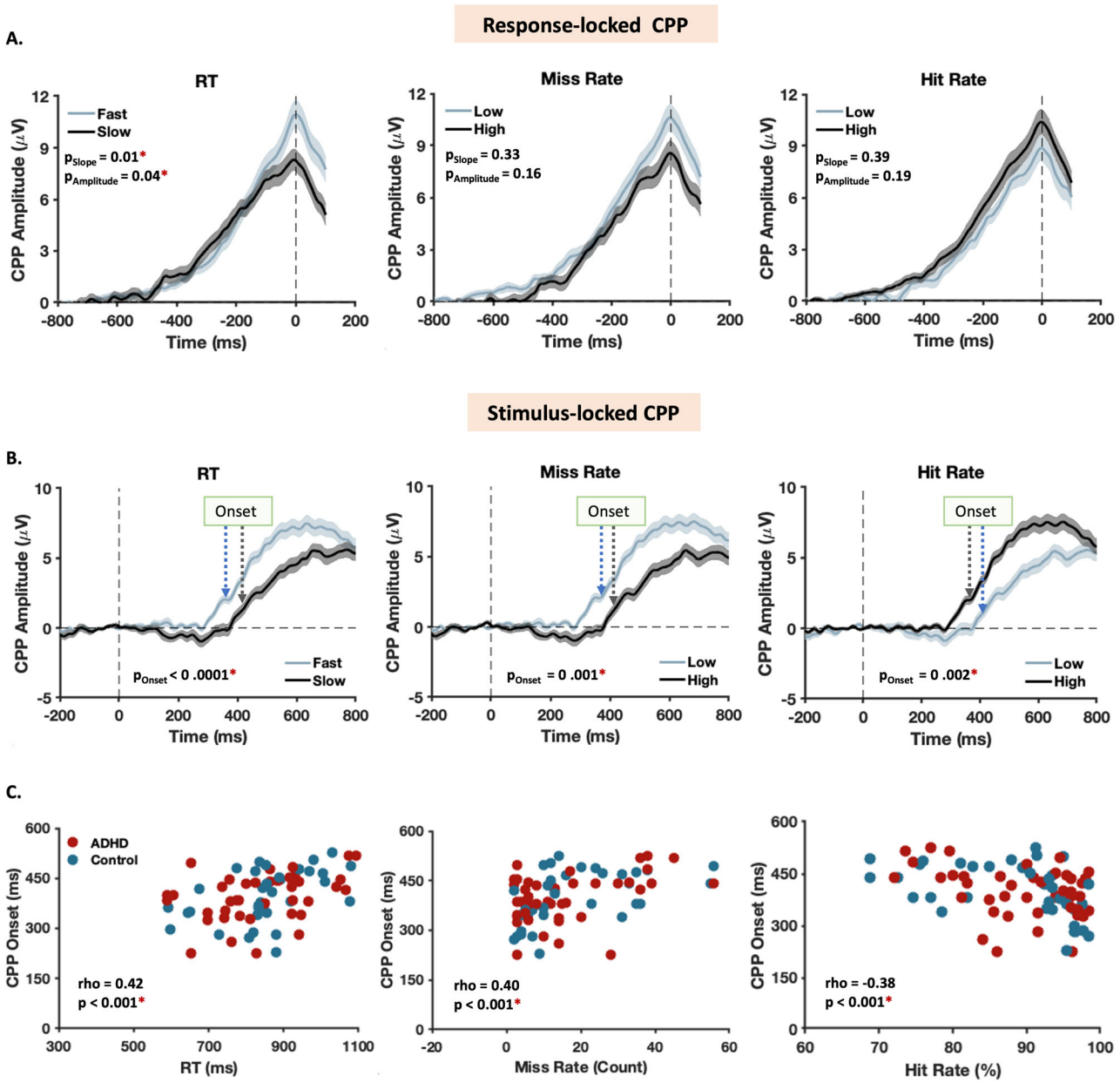

Figure 3. Relationship between CPP dynamics and performance. ***A***, ***B***, Differences in CPP signal between individuals with different levels of performance. CPP amplitude and slope are measured from the response-locked CPP (***A***) and CPP onset is from the stimulus-locked CPP (***B***). Participants are binned by the behavioral measure using a median split of the data. The thick line in the graph is the group-averaged waveform and the shaded areas represent changes in the standard error of mean over time. The vertical dashed lines marked "onset" compare the average onsets between the groups. P, *p* value from Wilcoxon signed rank test comparing the two groups. * indicates statistical significance ($p < 0.05$) in group difference. ***C***, The relationship between CPP onset (derived from the stimulus-locked CPP), which demonstrated significant predictive power for all behavioral measures and performance. *p* and r, *p* value and coefficient from partial Spearman's correlation analysis while controlling for group, age, and site.

of variations in this parameter and adding each of the EEG metrics significantly improved the model fit (alpha power: $R^2_{adj} = 0.14$, $F_{(4,74)} = 4.20$, $p = 0.004$; N2c latency: $R^2_{adj} = 0.19$, $F_{(5,73)} = 4.75$, $p < 0.001$; N2c amplitude: $R^2_{adj} = 0.18$, $F_{(6,72)} = 3.95$, $p = 0.002$; CPP onset: $R^2_{adj} = 0.24$, $F_{(7,71)} = 4.51$, $p < 0.001$; CPP slope: $R^2_{adj} = 0.23$, $F_{(8,70)} = 3.90$, $p < 0.001$; CPP amplitude: $R^2_{adj} = 0.22$, $F_{(9,69)} = 3.41$, $p = 0.002$; CNV slope: $R^2_{adj} = 0.21$, $F_{(10,68)} = 3.14$, $p = 0.002$; CNV amplitude: $R^2_{adj} = 0.22$, $F_{(11,67)} = 3.04$, $p = 0.002$) and only CPP onset (stand. $\beta = -0.31$, $t = -2.65$, $p = 0.01$) accounted for independent variation in response threshold.

The results above collectively provide evidence supporting associations between neural metrics of decision-making as measured with EEG and DDM parameters derived from behavioral outcomes. Among all EEG components, the dynamics of CPP emerged as the strongest contributor to the variations in DDM parameters.

Neurobehavioral characteristics of decision-making in ADHD

To investigate the distinctions in behavioral, DDM, and electrophysiological measures of decision-making between the ADHD and control groups, we conducted MANCOVA with site and age as covariates. As the Box's M test score was significant ($p < 0.001$), we used Pillai's trace statistic, which is considered to be most robust against type I error in MANCOVA (Olson, 1976; Scheiner, 2020). The results revealed significant main effects of group (Pillai's trace = 0.36, $F_{(14,\ 62)} = 2.50$, $p = 0.007$,

partial $\eta^2 = 0.36$) and age (Pillai's trace = 0.31, $F_{(14,\ 62)} = 1.98$, $p = 0.035$, partial $\eta^2 = 0.31$) but not site (Pillai's trace = 0.25, $F_{(14,\ 62)} = 1.48$, $p = 0.15$, partial $\eta^2 = 0.25$).

Table 1 summarizes pairwise comparisons of all the measures between the ADHD and control groups. Significant differences were observed between the two groups across all measures of performance, as well as the drift rate and response threshold parameters of DDM. All EEG components showed significant changes in ADHD in at least one feature of the signal, except for pretarget alpha. Figure 4 illustrates the differences in spatiotemporal patterns of EEG signals between the two groups.

Although CPP onset emerged as the strongest predictor of behavioral variations among all neural components, it did not significantly differ between groups. To determine whether the relationship between CPP onset and performance metrics was group specific, we conducted a post hoc analysis. Spearman's correlations (controlling for age and site) revealed that CPP onset was significantly correlated with all three performance measures in the control group (RT: rho = 0.4, $p = 0.01$; miss rate: rho = 0.56, $p < 0.001$; hit rate: rho = −0.50, $p = 0.001$) but only with RT in the ADHD group (RT: rho = 0.44, $p = 0.008$; miss rate: rho = 0.26, $p = 0.14$; hit rate: rho = −0.27, $p = 0.12$; Fig. 3). These findings suggest that, despite the overall significance of CPP onset, other critical factors—specifically altered in ADHD—obscure the brain–behavior relationships. Of note, Fisher's z-tests showed no statistically significant difference between the correlations (all p values > 0.05) in the two groups, suggesting this observation should be interpreted cautiously and explored further in future research.

Group differences in reaction time are mediated by variations in the neural measures of evidence accumulation

Given the predictive power of the CPP for decision-making performance and its capacity to distinguish between groups (CPP slope and amplitude), we tested whether CPP dynamics mediated the performance differences observed in ADHD. Because the mediation effects of the different CPP metrics were likely related, for each behavioral measure, we jointly tested all the three mediators in one model to assess simultaneous effects more accurately (MacKinnon et al., 2000, 2007). Bootstrapped mediation analyses with 5,000 samples (bias-corrected percentile; with site and age as confounding factors) revealed that the intersubject variation in RT for the ADHD group, at least in part, depends on individual differences in the efficiency of evidence accumulation (Table 2). The mediation effect was observed for CPP slope and amplitude, but not for CPP onset, which aligns with the lack of significant group-level differences in onset.

Finally, we sought to determine whether the EEG signatures could serve as predictors for the clinical scores. Hierarchical regression models revealed that variations in the EEG signatures collectively accounted for a significant portion of ∼70–80% (R^2_{adj}) variance in each clinical score. The model fit for each score was significantly improved by adding each neural metric (all $p_{\text{FDR-corrected}} < 0.001$). However, none of the EEG signals emerged as independent predictors for the clinical scores suggesting that these scores may reflect the interplay of multiple processing stages.

Table 1. Pairwise comparisons of measures between the ADHD and typically developing groups

Measures	Mean difference ADHD–Control	Std. error	Sig.	95% confidence interval	
RT (ms)	59.15	27.44	0.03[a]	4.48	113.815
Hit rate (%)	−3.73	1.66	0.03[a]	−7.04	−0.43
Miss rate (count)	7.74	2.86	0.008[a]	2.04	13.45
Drift rate (a.u.)	−0.72	0.28	0.01[a]	−1.28	−0.17
Nondecision Time (ms)	0.06	0.03	0.06	−0.002	0.13
Response threshold (a.u.)	−0.65	0.32	0.04[a]	−1.30	−0.02
Pretarget alpha [b] (μV^2)	−0.04	0.05	0.51	−0.14	0.07
N2c latency (ms)	−24.93	11.02	0.03[a]	−46.89	−2.98
N2c amplitude (μV)	0.75	0.33	0.02[a]	0.10	1.40
CPP onset (ms)	25.57	16.62	0.13	−7.54	58.68
CPP slope (μV/ms)	−0.006	0.002	0.01[a]	−0.01	−0.001
CPP amplitude (μV)	−2.35	0.86	0.008[a]	−4.06	−0.63
CNV slope (μV/ms)	0.02	0.009	0.03[a]	0.002	0.04
CNV amplitude (μV)	1.28	1.03	0.22	−0.77	3.33

[a]The mean difference is significant at an alpha level of 0.05, which survived following FDR correction for multiple comparisons in each category of measures (behavior, EEG, and DDM).
bMean values are multiplied by 10^{15}. Individual data points are presented in Extended Data Table 1-1.

Discussion

In this study, we aimed to develop a mechanistic account of ADHD-related changes in a fundamental cognitive process by integrating neurocognitive, neurophysiological, and computational levels of analysis and identified distinct phenotypic signatures. First, our findings confirmed the link between performance and the EEG signatures of cognitive processes during perceptual decision-making, highlighting CPP dynamics as robust, independent neural predictors across various measures (RT, miss rate, and hit rate). Also, consistent with the literature (Rommelse et al., 2007; Karalunas and Huang-Pollock, 2013), the ADHD cohort demonstrated significantly slower RTs, a higher number of missed targets, and a reduced hit rate. DDM parameters (drift rate and response threshold) also demonstrated sensitivity in distinguishing ADHD from typically developing children and were significantly correlated with neural dynamics of evidence accumulation (CPP). In addition, children with ADHD exhibited altered dynamics in several neurophysiological signatures of the decision process including target selection (early and attenuated N2c), evidence accumulation (reduced CPP slope and amplitude), and anticipation of voluntary action (reduced CNV slope). Critically, the interplay of these neural signals explained meaningful interindividual variation in performance and clinical outcomes.

The N2c component is a key signature of early target selection mechanisms that support the decision process by facilitating enhanced processing of target features (Loughnane et al., 2016). Although the marginally earlier latency of the N2c observed in children with ADHD could be interpreted as enhanced target detection, its diminished amplitude coupled with the poorer performance of the ADHD group more likely indicate premature processing of sensory information and/or changes in allocation of attentional resources. The N2c is closely related to the N2pc component elicited during visual search tasks, reflecting attentional impairment in ADHD, as indicated by altered timing and reduced amplitude (Cross-Villasana et al., 2015; Wang et al., 2016; Luo et al., 2019). Like the N2pc, the N2c functions as a general target selection signal emerging irrespective of the presence of distractors or the degree of spatiotemporal uncertainty (Loughnane et al., 2016). Although the N2c did not seem to act as an independent predictor of performance or clinical characteristics in ADHD, its significant contribution to models predicting behavioral outcomes and clinical scores suggests a partial link between ADHD-related decision-making impairments and the target selection mechanisms that support the decision process. N2c dynamics are relatively unexplored in

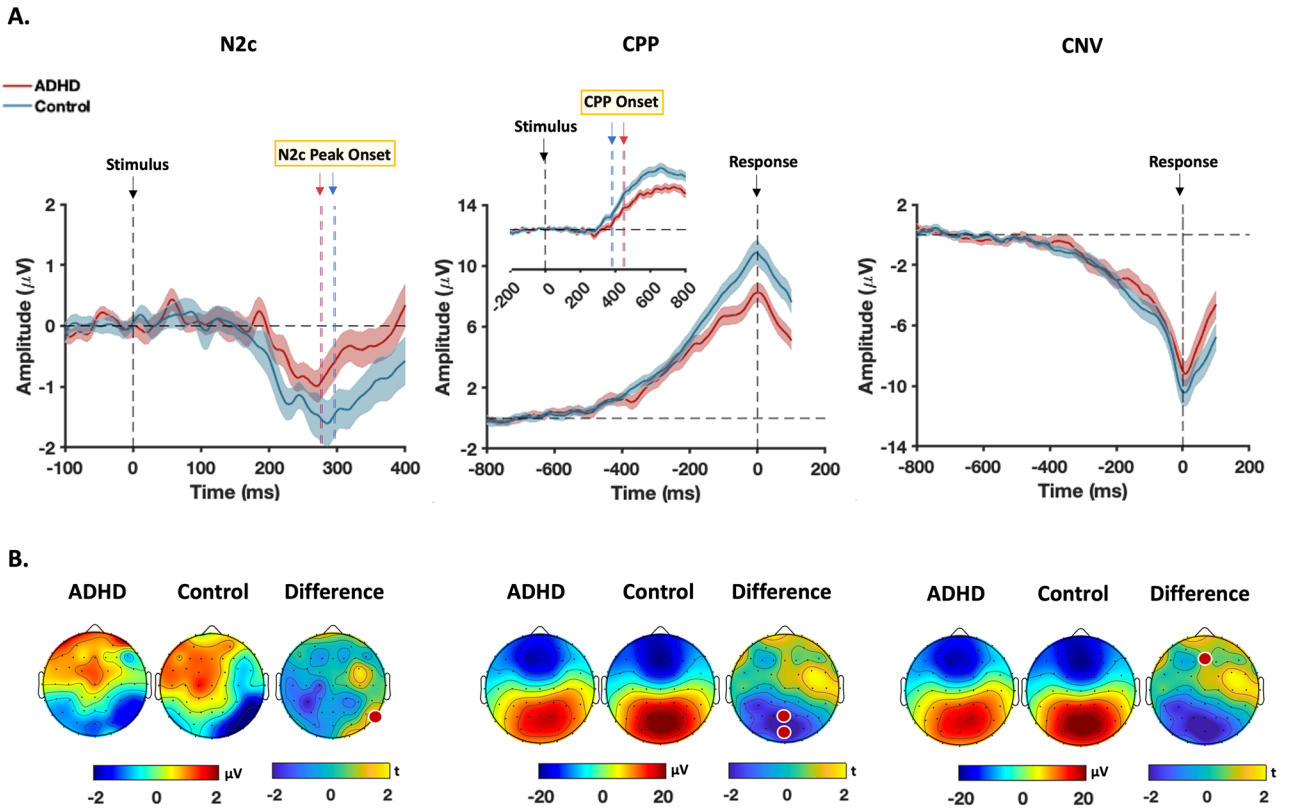

Figure 4. EEG signals of decision-making in ADHD and typically developing groups. ***A***, Group-averaged EEG signal waveforms for each neural signature of the decision process. The right graph illustrates the dynamics of N2c derived from the stimulus-locked signal contralateral to the target location recorded at P7 and P8. The middle graph displays the response-locked CPP, from which we derived measurements of CPP amplitude and slope. The inset graph depicts the stimulus-locked CPP, used to determine CPP onset. The left graph depicts the dynamics of CNV obtained from the response-locked signal recorded at FCz. The thick line in the graphs is the group-averaged waveform and the shaded areas represent the standard error of mean at each point of time. The vertical dashed line at the zero point indicates the onset of the target stimulus for N2c and the stimulus-locked CPP and represents the response time for the response-locked CPP and CNV. The horizontal dashed line represents the baseline level of EEG activity. The vertical dashed lines marked "onset" compare the average onsets between the groups. ***B***, The scalp maps depict the potential distribution for each group at the time of peak amplitude, and difference maps demonstrate the distribution of *t* values resulting from *t* tests comparing the two groups. The electrodes highlighted in red indicate the specific electrodes used for the line graphs and subsequent analysis. The scalp maps for CPP represent the response-locked signals used to measure amplitude. Statistical outcomes are detailed in Table 1.

Table 2. Mediation of CPP components on the impact of group on behavior

								95% confidence interval		
CPP components					Estimate	Std. error	*z* value	*p*	Lower	Upper
Group	→	Onset	→	RT	−0.08	0.05	−1.52	0.13	−0.20	0.02
Group	→	Slope	→	RT	−0.23	0.10	−2.31	0.02*	−0.44	−0.07
Group	→	Amplitude	→	RT	0.17	0.08	2.18	0.03*	0.03	0.37
Group	→	Onset	→	MR	−0.06	0.04	−1.45	0.15	−0.19	0.01
Group	→	Slope	→	MR	−0.03	0.06	−0.51	0.61	−0.21	0.11
Group	→	Amplitude	→	MR	0.01	0.06	0.13	0.90	−0.16	0.15
Group	→	Onset	→	HR	0.06	0.04	1.43	0.15	−0.01	0.18
Group	→	Slope	→	HR	0.05	0.06	0.81	0.42	−0.06	0.21
Group	→	Amplitude	→	HR	−0.02	0.06	−0.35	0.73	−0.17	0.11

RT, reaction time; MR, miss rate; HR, hit rate. * statistical significance. Note: the results are from three separate models for the three behavioral measures.

the ADHD literature and, given the importance of attentional differences to ADHD, merit further investigation.

There is evidence that a key mechanism that changes in ADHD may be the rate of basic information processing (Rommelse et al., 2007; Salum et al., 2014a,b; Mihali et al., 2018). Indeed, efforts to model a variety of behavioral impairments associated with ADHD have consistently highlighted the rate of evidence accumulation as the core contributor to performance changes (Karalunas et al., 2012, 2014; Huang-Pollock et al., 2017, 2020; Weigard and Sripada, 2021). In line with prior computational modeling studies across various neurocognitive paradigms (Shapiro and Huang-Pollock, 2019; Weigard and Sripada, 2021), we found a significant attenuation in the DDM drift rate parameter in individuals with ADHD. Our EEG findings complement this work by tracing the dynamics of an established neurophysiological index of evidence accumulation, the CPP. CPP dynamics (onset) not only exhibited robust predictive power for all the measures of cognitive performance

examined in this study but also differed significantly between ADHD and typically developing individuals (CPP slope and amplitude). Although CPP onset was delayed in the ADHD group, this difference did not reach statistical significance. This result, coupled with the apparent weakened relationship observed between CPP onset and behavior in the ADHD group, might reflect underlying complexities in the neural dynamics of ADHD, though this difference was not statistically significant. It is likely that our trial-averaged approach has obscured variations in neural timing and amplitude, particularly in ADHD, where such variability is expected to be higher. This smearing effect can blur the precise timing and reduce the perceived strength of neural signals, which prevents the accurate detection of CPP onset, making it more difficult to detect its true relationship with behavior. A trial-wise approach that captures both amplitude and timing variations more effectively could potentially clarify such changes in brain–behavior relationships in ADHD. In line with claims of inefficient evidence accumulation in ADHD, we found a reduced CPP slope and a smaller CPP amplitude in the ADHD group. More consistent with previous research showing that steeper CPP slopes predict faster reaction times and CPP amplitude is reliably greater for hits than for misses (O'Connell et al., 2012; Kelly and O'Connell, 2013, 2015), this result provides neurophysiological evidence to support the hypothesis that suboptimal evidence accumulation or poorer signal-to-noise ratios in the processing of task-relevant information may contribute to differences in decision-making in ADHD.

While both CPP slope and DDM drift rate are suggested to reflect the rate of evidence accumulation, we found drift rate was independently predicted by CPP onset, not slope. Despite this, the inclusion of CPP slope in the regression significantly improved the model fit. These results suggest that the two metrics do correlate, but the contribution of CPP slope to drift rate is shared with other neural predictors in the model. This agrees with previous literature, which indicates that CPP slope is influenced by earlier neural processes in decision-making, such as attentional engagement (alpha power; Kelly and O'Connell, 2013) and attentional selection (N2 amplitude; Loughnane et al., 2016). CNV amplitude is also expected to covary with CPP slope, with larger CPP slopes associated with smaller CNVs due to faster RTs and less time for urgency to grow. Our data confirms that CPP slope covaries with both alpha power (rho = 0.24, $p = 0.04$) and CNV amplitude (rho = −0.34, $p = 0.003$). Therefore, these neural metrices probably share some of the variance contributed by CPP slope, making it difficult for CPP slope to account for unique variance independently. Overall, these findings suggest that CPP may not be a direct neural analog to the DDM drift rate.

The strong predictive power of CPP onset for drift rate may, in part, be due to methodological constraints in onset detection. CPP onset is identified at the point where the signal reliably exceeds background noise, and this measurement may be influenced by the rate of evidence accumulation. Participants with faster accumulation rates could surpass the noise threshold earlier, leading to earlier detected onsets. Therefore, while we cannot rule out that drift rate and CPP onset are dependent, there is a possibility that their true relationship has been obscured by methodological limitations.

To our knowledge, this study is the first to investigate CPP dynamics in ADHD. However, the P300 event-related potential [the CPP is typically observed during extended perceptual discrimination, while the P300 is evoked by discrete sensory events (e.g., an oddball stimulus); Twomey et al., 2015; O'Connell and Kelly, 2021], also associated with evidence accumulation, has consistently been reported to have reduced amplitude in ADHD across a variety of tasks (Itagaki et al., 2011; Hasler et al., 2016; Kaiser et al., 2020). In fact, these effects are sufficiently robust that P300 dynamics have been proposed as potential ADHD biomarkers (Kaiser et al., 2020) and metrics for research on pharmacological treatment (Ogrim et al., 2016; Yamamuro et al., 2016; Peisch et al., 2021). Although the interpretation of these P300 effects varies across tasks, these results can be broadly characterized as reflecting suboptimal processing of task-relevant information. The CPP is thought to be functionally equivalent to the P300 (Itagaki et al., 2011), but studying the CPP offers several critical advantages over this previous work. Unlike the stimulus-locked P300, the slope and amplitude of CPP are estimated from the response-locked potentials accounting for the fact that the signal peaks at the time of response. Furthermore, the P300 analysis often overlooks the onset and build-up rate of the signal which are critical for understanding the neural processes underlying evidence accumulation.

The present findings also align with research that indicates methylphenidate (MPH) enhances cognitive task performance by improving evidence accumulation. MPH is the mainstay treatment for ADHD and has been shown to normalize the reduced DDM drift rate in ADHD (Fosco et al., 2017). It also realigns P300 dynamics in neurocognitive (Peisch et al., 2021) and perceptual decision-making tasks (Loughnane et al., 2019). Additionally, preliminary evidence suggests that MPH enhances CPP slope in human EEG (Loughnane et al., 2019). The neural mechanisms by which MPH might enhance evidence accumulation are still largely unknown although some evidence from behavioral modeling studies suggests that it may regulate the suboptimal neural signal-to-noise ratios in children with ADHD (Ratcliff et al., 2009; Loughnane et al., 2019; Pertermann et al., 2019), suggesting that an increase in neural gain may account for effects observed on the P300. Future studies may yield a deeper understanding of the pharmacology of discrete processing stages underlying human choice behavior by integrating the EEG paradigms and computational modeling approach employed in the present study with pharmacological manipulation.

Finally, our data revealed ADHD-related changes in CNV dynamics, which also contributed to the variation in behavioral performance. The CNV signal is commonly observed in target detection and choice response time tasks, which is associated with temporal preparation for anticipated events or volitional movements (Brunia and Van Boxtel, 2001; Van Rijn et al., 2011; Baker et al., 2012). This signal is influenced by dopaminergic systems (Birbaumer et al., 1990) and its attenuation has been widely reported in children (Banaschewski et al., 2003; Doehnert et al., 2013; Kaiser et al., 2020) and adults with ADHD (McLoughlin et al., 2010, 2011; Hasler et al., 2016). Indeed, this signal has been suggested as a robust neurophysiological marker of ADHD which effectively captures the underlying deficits in their preparatory motor processes (Doehnert et al., 2013; Kaiser et al., 2020). In the context of perceptual decision-making, the CNV is also described as a neural index of urgency which grows in a time-dependent but evidence-independent manner reflecting speed pressure in response (Devine et al., 2019). Given the slowed evidence accumulation in the ADHD group, one might expect an increased urgency to reach decision commitments as a compensatory mechanism. It appears that such strategic adjustment was not adaptive here as the ADHD group demonstrated poorer performance on average. This finding,

along with the observed reduction in decision threshold in ADHD, may provide further evidence supporting that they may have inefficient adjustment in the inherent speed/accuracy trade-off in response to task demands (Mulder et al., 2010). It is possible that dysregulation of the timing mechanism associated with the CNV may contribute to this relative maladaptation.

Our findings establish links between EEG metrics of decision-making, behavior, and DDM parameters in children with and without ADHD. Future studies should confirm these relationships in diverse cohorts to strengthen the robustness and generalizability of our results. The present study also provides novel neurophysiological evidence linking differences in decision-making in ADHD to alterations in the dynamics and interplay of the neural signals indexing three key cognitive processes: target selection, decision formation, and dynamic urgency. The results provide an integrated account of these changes, identifying neural signals with the potential to explain diverse performance profiles in ADHD and to inform personalized treatment approaches. These neural markers can also serve as critical guidance in constructing or constraining mechanistic accounts in future ADHD research. Crucially, the altered relationship between specific neural signals and behavior in ADHD may uncover unexplored mechanisms underlying decision-making processes, warranting further in-depth investigation.

Data Availability

Our custom-developed EEG pipeline, including the preprocessing steps and extraction of the EEG metrics, along with our code for DDM of the behavioral data, is available at https://github.com/ManaBiabani/DM_ADHD.

References

Baker KS, Piriyapunyaporn T, Cunnington R (2012) Neural activity in readiness for incidental and explicitly timed actions. Neuropsychologia 50: 715–722.

Banaschewski T, Brandeis D, Heinrich H, Albrecht B, Brunner E, Rothenberger A (2003) Association of ADHD and conduct disorder–brain electrical evidence for the existence of a distinct subtype. J Child Psychol Psychiatry 44:356–376.

Barkley RA (1997) Behavioral inhibition, sustained attention, and executive functions: constructing a unifying theory of ADHD. Psychol Bull 121:65.

Bellgrove MA, Hawi Z, Kirley A, Gill M, Robertson IH (2005) Dissecting the attention deficit hyperactivity disorder (ADHD) phenotype: sustained attention, response variability and spatial attentional asymmetries in relation to dopamine transporter (DAT1) genotype. Neuropsychologia 43: 1847–1857.

Birbaumer N, Elbert T, Canavan AG, Rockstroh B (1990) Slow potentials of the cerebral cortex and behavior. Physiol Rev 70:1–41.

Brainard DH, Vision S (1997) The psychophysics toolbox. Spat Vis 10:433–436.

Brosnan M, Pearce DJ, O'Neill MH, Loughnane GM, Fleming B, Zhou S-H, Chong T, Nobre AC, Connell RG, Bellgrove MA (2023) Evidence accumulation rate moderates the relationship between enriched environment exposure and age-related response speed declines. J Neurosci 43: 6401–6414.

Brosnan MB, Sabaroedin K, Silk T, Genc S, Newman DP, Loughnane GM, Fornito A, O'Connell RG, Bellgrove MA (2020) Evidence accumulation during perceptual decisions in humans varies as a function of dorsal frontoparietal organization. Nat Hum Behav 4:844–855.

Brunia C, Van Boxtel G (2001) Wait and see. Int J Psychophysiol 43:59–75.

Coghill DR, Seth S, Matthews K (2014) A comprehensive assessment of memory, delay aversion, timing, inhibition, decision making and variability in attention deficit hyperactivity disorder: advancing beyond the three-pathway models. Psychol Med 44:1989–2001.

Cross-Villasana F, Finke K, Hennig-Fast K, Kilian B, Wiegand I, Müller HJ, Möller H-J, Töllner T (2015) The speed of visual attention and motor-response decisions in adult attention-deficit/hyperactivity disorder. Biol Psychiatry 78:107–115.

de Gee JW, Tsetsos K, Schwabe L, Urai AE, McCormick D, McGinley MJ, Donner TH (2020) Pupil-linked phasic arousal predicts a reduction of choice bias across species and decision domains. Elife 9:e54014.

Delorme A, Makeig S (2004) EEGLAB: an open source toolbox for analysis of single-trial EEG dynamics including independent component analysis. J Neurosci Methods 134:9–21.

Devine CA, Gaffney C, Loughnane GM, Kelly SP, O'Connell RG (2019) The role of premature evidence accumulation in making difficult perceptual decisions under temporal uncertainty. Elife 8:e48526.

Doehnert M, Brandeis D, Schneider G, Drechsler R, Steinhausen H (2013) A neurophysiological marker of impaired preparation in an 11-year follow-up study of attention-deficit/hyperactivity disorder (ADHD). J Child Psychol Psychiatry 54:260–270.

Forstmann BU, Ratcliff R, Wagenmakers E-J (2016) Sequential sampling models in cognitive neuroscience: advantages, applications, and extensions. Annu Rev Psychol 67:641–666.

Fosco WD, White CN, Hawk LW (2017) Acute stimulant treatment and reinforcement increase the speed of information accumulation in children with ADHD. J Abnorm Child Psychol 45:911–920.

Foxe JJ, Simpson GV (2002) Flow of activation from V1 to frontal cortex in humans: a framework for defining "early" visual processing. Exp Brain Res 142:139–150.

Gold JI, Shadlen MN (2007) The neural basis of decision making. Annu Rev Neurosci 30:535–574.

Gonen-Yaacovi G, Arazi A, Shahar N, Karmon A, Haar S, Meiran N, Dinstein I (2016) Increased ongoing neural variability in ADHD. Cortex 81:50–63.

Goulardins JB, Marques JC, De Oliveira JA (2017) Attention deficit hyperactivity disorder and motor impairment: a critical review. Percept Mot Skills 124:425–440.

Hanks TD, Summerfield C (2017) Perceptual decision making in rodents, monkeys, and humans. Neuron 93:15–31.

Hasler R, Perroud N, Meziane HB, Herrmann F, Prada P, Giannakopoulos P, Deiber MP (2016) Attention-related EEG markers in adult ADHD. Neuropsychologia 87:120–133.

Huang-Pollock CL, Karalunas SL, Tam H, Moore AN (2012) Evaluating vigilance deficits in ADHD: a meta-analysis of CPT performance. J Abnorm Psychol 121:360.

Huang-Pollock C, Ratcliff R, McKoon G, Roule A, Warner T, Feldman J, Wise S (2020) A diffusion model analysis of sustained attention in children with attention deficit hyperactivity disorder. Neuropsychology 34:641.

Huang-Pollock C, Ratcliff R, McKoon G, Shapiro Z, Weigard A, Galloway-Long H (2017) Using the diffusion model to explain cognitive deficits in attention deficit hyperactivity disorder. J Abnorm Child Psychol 45:57–68.

Hurks P, Adam J, Hendriksen J, Vles J, Feron F, Kalff A, Kroes M, Steyaert J, Crolla I, van Zeben T (2005) Controlled visuomotor preparation deficits in attention-deficit/hyperactivity disorder. Neuropsychology 19:66.

Itagaki S, Yabe H, Mori Y, Ishikawa H, Takanashi Y, Niwa S (2011) Event-related potentials in patients with adult attention-deficit/hyperactivity disorder versus schizophrenia. Psychiatry Res 189:288–291.

Johnson KA, Kelly SP, Bellgrove MA, Barry E, Cox M, Gill M, Robertson IH (2007) Response variability in attention deficit hyperactivity disorder: evidence for neuropsychological heterogeneity. Neuropsychologia 45: 630–638.

Kaiser A, Aggensteiner P-M, Baumeister S, Holz NE, Banaschewski T, Brandeis D (2020) Earlier versus later cognitive event-related potentials (ERPs) in attention-deficit/hyperactivity disorder (ADHD): a meta-analysis. Neurosci Biobehav Rev 112:117–134.

Kaiser ML, Schoemaker M, Albaret J-M, Geuze R (2015) What is the evidence of impaired motor skills and motor control among children with attention deficit hyperactivity disorder (ADHD)? Systematic review of the literature. Res Dev Disabil 36:338–357.

Karalunas SL, Geurts HM, Konrad K, Bender S, Nigg JT (2014) Reaction time variability in ADHD and autism spectrum disorders: measurement and mechanisms of a proposed trans-diagnostic phenotype. J Child Psychol Psychiatry 55:685–710.

Karalunas SL, Hawkey E, Gustafsson H, Miller M, Langhorst M, Cordova M, Fair D, Nigg JT (2018) Overlapping and distinct cognitive impairments in attention-deficit/hyperactivity and autism spectrum disorder without intellectual disability. J Abnorm Child Psychol 46:1705–1716.

Karalunas SL, Huang-Pollock CL (2013) Integrating impairments in reaction time and executive function using a diffusion model framework. J Abnorm Child Psychol 41:837–850.
Karalunas SL, Huang-Pollock CL, Nigg JT (2012) Decomposing attention-deficit/hyperactivity disorder (ADHD)-related effects in response speed and variability. Neuropsychology 26:684.
Kelly SP, O'Connell RG (2013) Internal and external influences on the rate of sensory evidence accumulation in the human brain. J Neurosci 33: 19434–19441.
Kelly SP, O'Connell RG (2015) The neural processes underlying perceptual decision making in humans: recent progress and future directions. J Physiol-Paris 109:27–37.
Kim S, Chen S, Tannock R (2014) Visual function and color vision in adults with attention-deficit/hyperactivity disorder. J Optom 7:22–36.
Loughnane GM, Brosnan MB, Barnes JJ, Dean A, Nandam SL, O'Connell RG, Bellgrove MA (2019) Catecholamine modulation of evidence accumulation during perceptual decision formation: a randomized trial. J Cogn Neurosci 31:1044–1053.
Loughnane GM, Newman DP, Bellgrove MA, Lalor EC, Kelly SP, O'Connell RG (2016) Target selection signals influence perceptual decisions by modulating the onset and rate of evidence accumulation. Curr Biol 26:496–502.
Luo X, Guo J, Liu L, Zhao X, Li D, Li H, Zhao Q, Wang Y, Qian Q, Wang Y (2019) The neural correlations of spatial attention and working memory deficits in adults with ADHD. NeuroImage Clin 22:101728.
MacKinnon DP, Fairchild AJ, Fritz MS (2007) Mediation analysis. Annu Rev Psychol 58:593–614.
MacKinnon DP, Krull JL, Lockwood CM (2000) Equivalence of the mediation, confounding and suppression effect. Prev Sci 1:173–181.
McGovern DP, Hayes A, Kelly SP, O'Connell RG (2018) Reconciling age-related changes in behavioural and neural indices of human perceptual decision-making. Nat Hum Behav 2:955–966.
McLoughlin G, Albrecht B, Banaschewski T, Rothenberger A, Brandeis D, Asherson P, Kuntsi J (2010) Electrophysiological evidence for abnormal preparatory states and inhibitory processing in adult ADHD. Behav Brain Funct 6:1–12.
McLoughlin G, Asherson P, Albrecht B, Banaschewski T, Rothenberger A, Brandeis D, Kuntsi J (2011) Cognitive-electrophysiological indices of attentional and inhibitory processing in adults with ADHD: familial effects. Behav Brain Funct 7:1–9.
Mihali A, Young AG, Adler LA, Halassa MM, Ma WJ (2018) A low-level perceptual correlate of behavioral and clinical deficits in ADHD. Comput Psychiatry Camb Mass 2:141.
Mowinckel AM, Pedersen ML, Eilertsen E, Biele G (2015) A meta-analysis of decision-making and attention in adults with ADHD. J Atten Disord 19: 355–367.
Mulder MJ, Bos D, Weusten JM, van Belle J, van Dijk SC, Simen P, van Engeland H, Durston S (2010) Basic impairments in regulating the speed-accuracy tradeoff predict symptoms of attention-deficit/hyperactivity disorder. Biol Psychiatry 68:1114–1119.
Myers CE, Interian A, Moustafa AA (2022) A practical introduction to using the drift diffusion model of decision-making in cognitive psychology, neuroscience, and health sciences. Front Psychol 13:1039172.
Nigg JT (2013) Attention-deficit/hyperactivity disorder and adverse health outcomes. Clin Psychol Rev 33:215–228.
O'Connell RG, Dockree PM, Kelly SP (2012) A supramodal accumulation-to-bound signal that determines perceptual decisions in humans. Nat Neurosci 15:1729–1735.
O'Connell RG, Kelly SP (2021) Neurophysiology of human perceptual decision-making. Annu Rev Neurosci 44:495–516.
O'Connell RG, Shadlen MN, Wong-Lin K, Kelly SP (2018) Bridging neural and computational viewpoints on perceptual decision-making. Trends Neurosci 41:838–852.
Ogrim G, Aasen IE, Brunner JF (2016) Single-dose effects on the P3no-go ERP component predict clinical response to stimulants in pediatric ADHD. Clin Neurophysiol 127:3277–3287.
Olson CL (1976) On choosing a test statistic in multivariate analysis of variance. Psychol Bull 83:579.
Panagiotidi M, Overton PG, Stafford T (2018) The relationship between ADHD traits and sensory sensitivity in the general population. Compr Psychiatry 80:179–185.
Peisch V, Rutter T, Wilkinson CL, Arnett AB (2021) Sensory processing and P300 event-related potential correlates of stimulant response in children with attention-deficit/hyperactivity disorder: a critical review. Clin Neurophysiol 132:953–966.
Pennington BF, Ozonoff S (1996) Executive functions and developmental psychopathology. J Child Psychol Psychiatry 37:51–87.
Pertermann M, Bluschke A, Roessner V, Beste C (2019) The modulation of neural noise underlies the effectiveness of methylphenidate treatment in attention-deficit/hyperactivity disorder. Biol Psychiatry Cogn Neurosci Neuroimaging 4:743–750.
Powell MJ (1964) An efficient method for finding the minimum of a function of several variables without calculating derivatives. Comput J 7:155–162.
Ratcliff R, Huang-Pollock C, McKoon G (2018) Modeling individual differences in the go/no-go task with a diffusion model. Decision 5:42.
Ratcliff R, McKoon G (2008) The diffusion decision model: theory and data for two-choice decision tasks. Neural Comput 20:873–922.
Ratcliff R, Philiastides MG, Sajda P (2009) Quality of evidence for perceptual decision making is indexed by trial-to-trial variability of the EEG. Proc Natl Acad Sci 106:6539–6544.
Ratcliff R, Smith PL, Brown SD, McKoon G (2016) Diffusion decision model: current issues and history. Trends Cogn Sci 20:260–281.
Rommelse NN, Altink ME, de Sonneville LM, Buschgens CJ, Buitelaar J, Oosterlaan J, Sergeant JA (2007) Are motor inhibition and cognitive flexibility dead ends in ADHD? J Abnorm Child Psychol 35:957–967.
Rommelse NN, Altink ME, Oosterlaan J, Beem L, Buschgens CJ, Buitelaar J, Sergeant JA (2008) Speed, variability, and timing of motor output in ADHD: which measures are useful for endophenotypic research? Behav Genet 38:121–132.
Salum G, Sergeant J, Sonuga-Barke E, Vandekerckhove J, Gadelha A, Pan P, Moriyama T, Graeff-Martins A, de Alvarenga PG, Do Rosário M (2014a) Specificity of basic information processing and inhibitory control in attention deficit hyperactivity disorder. Psychol Med 44: 617–631.
Salum G, Sonuga-Barke E, Sergeant J, Vandekerckhove J, Gadelha A, Moriyama T, Graeff-Martins A, Manfro G, Polanczyk G, Rohde L (2014b) Mechanisms underpinning inattention and hyperactivity: neurocognitive support for ADHD dimensionality. Psychol Med 44: 3189–3201.
Scheiner SM (2020) MANOVA: multiple response variables and multispecies interactions. In: *Design and analysis of ecological experiments* (Scheiner SM, Gurevitch J, eds), pp 94–112. New York: Chapman and Hall/CRC.
Sciberras E, Streatfeild J, Ceccato T, Pezzullo L, Scott JG, Middeldorp CM, Hutchins P, Paterson R, Bellgrove MA, Coghill D (2022) Social and economic costs of attention-deficit/hyperactivity disorder across the lifespan. J Atten Disord 26:72–87.
Sergeant JA, Geurts H, Huijbregts S, Scheres A, Oosterlaan J (2003) The top and the bottom of ADHD: a neuropsychological perspective. Neurosci Biobehav Rev 27:583–592.
Sergeant JA, Geurts H, Oosterlaan J (2002) How specific is a deficit of executive functioning for attention-deficit/hyperactivity disorder? Behav Brain Res 130:3–28.
Shapiro Z, Huang-Pollock C (2019) A diffusion-model analysis of timing deficits among children with ADHD. Neuropsychology 33:883.
Stefanac NR, Zhou SH, Spencer-Smith MM, O'Connell R, Bellgrove MA (2021) A neural index of inefficient evidence accumulation in dyslexia underlying slow perceptual decision making. Cortex 142:122–137.
Steinemann NA, O'Connell RG, Kelly SP (2018) Decisions are expedited through multiple neural adjustments spanning the sensorimotor hierarchy. Nat Commun 9:3627.
Twomey DM, Murphy PR, Kelly SP, O'Connell RG (2015) The classic P300 encodes a build-to-threshold decision variable. Eur J Neurosci 42:1636–1643.
Van Rijn H, Kononowicz TW, Meck WH, Ng KK, Penney TB (2011) Contingent negative variation and its relation to time estimation: a theoretical evaluation. Front Integr Neurosci 5:91.
Wang E, Sun L, Sun M, Huang J, Tao Y, Zhao X, Wu Z, Ding Y, Newman DP, Bellgrove MA (2016) Attentional selection and suppression in children with attention-deficit/hyperactivity disorder. Biol Psychiatry Cogn Neurosci Neuroimaging 1:372–380.
Weigard A, Sripada C (2021) Task-general efficiency of evidence accumulation as a computationally defined neurocognitive trait: implications for clinical neuroscience. Biol Psychiatry Glob Open Sci 1:5–15.

Wiecki TV, Sofer I, Frank MJ (2013) HDDM: hierarchical Bayesian estimation of the drift-diffusion model in python. Front Neuroinform 7:14.
Willcutt EG, Doyle AE, Nigg JT, Faraone SV, Pennington BF (2005) Validity of the executive function theory of attention-deficit/hyperactivity disorder: a meta-analytic review. Biol Psychiatry 57:1336–1346.
Yamamuro K, Ota T, Iida J, Nakanishi Y, Matsuura H, Uratani M, Okazaki K, Kishimoto N, Tanaka S, Kishimoto T (2016) Event-related potentials reflect the efficacy of pharmaceutical treatments in children and adolescents with attention deficit/hyperactivity disorder. Psychiatry Res 242:288–294.
Yau Y, Hinault T, Taylor M, Cisek P, Fellows LK, Dagher A (2021) Evidence and urgency related EEG signals during dynamic decision-making in humans. J Neurosci 41:5711–5722.
Zhou SH, Loughnane G, O'Connell R, Bellgrove MA, Chong TTJ (2021) Distractors selectively modulate electrophysiological markers of perceptual decisions. J Cogn Neurosci 33:1020–1031.